Factors Influencing the Configuration and Conformation of Diamine Chelate Rings in Platinum(II) Compounds: 2,4-Bis(methylamino)pentane Complexes

Leonardo Cerasino,[†] Kevin M. Williams,[‡] Francesco P. Intini,[†] Renzo Cini,[§] Luigi G. Marzilli,*[,‡] and Giovanni Natile*[,†]

Dipartimento Farmaco-Chimico, Università di Bari, via E. Orabona 4, 70125 Bari, Italy, Department of Chemistry, Emory University, Atlanta, Georgia 30322, and Dipartimento di Scienze e Tecnologie Chimiche e dei Biosistemi, Università di Siena, Pian dei Mantellini 44, 53100 Siena, Italy

Received June 6, 1997[⊗]

Complexes of the type $[PtX_2(Me_2DAP)]$ (Me_2DAP = 2,4-bis(methylamino)pentane) have been prepared and studied by ^1H NMR spectroscopy, molecular mechanics/dynamics (MMD) calculations, and X-ray crystallography. The coordinated Me_2DAP ligand has four asymmetric centers. Complexes with an enantiomeric form of the ligand (e.g., *RR*-Me_2DAP, *RR* being the configurations of the two asymmetric carbons) have three possible configurations, namely, *SRRR*, *RRRR*, and *SRRS* at N, C, C, and N, respectively. Indeed these three isomers were obtained in respective ratios of 9:1:∼0 for $X = I^-$ and of 7:3:1 for $X = Cl^-$. Complexes with the meso ligand (*RS*-Me_2DAP) have four possible configurations, i.e., *SRSR*, *RRSS*, *RRSR*, and *SRSS* at N, C, C, and N, respectively (the latter two constitute an enantiomeric pair). Only the two symmetrical isomers were obtained in the ratios of 9:1 for $X = I^-$ and 1:1 for $X = Cl^-$. In addition, the preferred chelate ring conformations in solution ($CDCl_3$) were determined to be the following: δ-chair (*SRRR*), λ-skew (*RRRR*), fluxional chair (*SRRS*), fluxional skew (*SRSR*), and λ-chair (*RRSS*). This information was used to assess the contributions of intra- and interligand interactions to determine the conformational stability. MMD calculations employing the AMBER force field [as modified by Yao et al. (Yao, S.; Plastaras, J. P.; Marzilli, L. G. *Inorg. Chem.* **1994**, *33*, 6061) and extended to include parameters for the Cl^- ligands] provided minimum-energy structures for all five $X = Cl^-$ complexes. These structures agreed well with the experimentally determined solution conformations except for *SRSR*, which had a lowest energy δ-chair instead of skew conformation. X-ray structural studies of the *SRSR* species ($X = Cl^-$ and $X = I^-$) confirmed the δ-chair conformation. The results suggest that an equatorial *N*-methyl group has nonbonded clashes with the *cis* chloride ligand; therefore, axial *N*-methyl groups are favored. However, in solution, the solvent and entropy (connected with fluxionality of conformers) are factors which, to some degree, can overcome the interligand steric interaction.

Introduction

The dependence of biological activity on the structure of platinum complexes with enantiomeric amine ligands such as $[PtCl_2$(*RR*-DACH)] and $[PtCl_2$(*SS*-DACH)] (DACH = 1,2-diaminocyclohexane)[1] and other enantiomeric pairs[2,3] has been the focus of considerable interest. However, in only very few cases does the asymmetry involve an N-donor atom. Platinum compounds with chiral diamine ligands could interact stereospecifically with DNA and even with mononucleotides.[4]

Nitrogen stereo centers in amine ligands invert readily unless coordinated to a metal such as platinum.[5] Coordination of unresolved amine ligands with chiral nitrogen stereo centers leads to a distribution of enantiomeric pairs of isomers which are difficult to resolve because platinum anticancer compounds are neutral. One way to circumvent this difficulty is the use of didentate ligands in which there are also chiral centers in the C backbone, the aim being that the chirality on the carbons could influence both the puckering of the chelate ring and the stereochemistry on the nitrogen.

cis-DDP cross-links purine residues of DNA in the head-to-head (HH)[6] and head-to-tail (HT)[7] conformations in which both H8 atoms are on the same and opposite sides of the platinum coordination plane, respectively. For DNA, HH is most common, but if the two nucleotide moieties are not linked by a

* Corresponding authors. E-mail: natile@farm.uniba.it; lmarzil@emory.edu.
[†] Università di Bari.
[‡] Emory University.
[§] Università di Siena.
[⊗] Abstract published in *Advance ACS Abstracts,* November 1, 1997.

(1) Kidani, Y.; Inagaki, K.; Saito, R.; Tsukagoshi, S. *J. Clin. Hematol. Oncol.* **1977**, *7*, 197. Kidani, Y.; Inagaki, K.; Iigo, M.; Hoshi, A.; Kuretani, K. *J. Med. Chem.* **1978**, *21*, 1315. Kidani, Y.; Noji, M.; Tashior, T. *Gann* **1980**, *71*, 637. Noji, M.; Okamato, K.; Kidani, Y.; Tashiro, T. *J. Med. Chem.* **1981**, *24*, 508.
(2) Noji, M.; Motoyama, S.; Tashiro, T.; Kidani, Y. *Chem. Pharm. Bull.* **1983**, *31*, 1469.
(3) Coluccia, M.; Correale, M.; Giordano, D.; Mariggiò, M. A.; Moscelli, S.; Fanizzi, F. P.; Natile, G.; Maresca, L. *Inorg. Chim. Acta* **1986**, *123*, 225. Coluccia, M.; Fanizzi, F. P.; Giannini, G.; Giordano, D.; Intini, F. P.; Lacidogna, G.; Loseto, F.; Mariggiò, M. A.; Nassi, A.; Natile, G. *Anticancer Res.* **1991**, *11*, 281. Giannini, G.; Natile, G. *Inorg. Chem.* **1991**, *30*, 2853. Fanizzi, F. P.; Intini, F. P.; Maresca, L.; Natile, G.; Quaranta, R.; Coluccia, M.; Dibari, L.; Giordano, D.; Mariggiò, M. A. *Inorg. Chim. Acta* **1987**, *137*, 45.
(4) Kiser, D.; Intini, F. P.; Xu, Y.; Natile, G.; Marzilli, L. G. *Inorg. Chem.* **1994**, *33*, 4149.
(5) Buckingham, D. A.; Marzilli, L. G.; Sargeson, A. M. *J. Am. Chem. Soc.* **1969**, *91*, 5227.
(6) Fichtinger-Schepman, A. M. J.; van der Veer, J. L.; den Hartog, J. H. J.; Lohman, P. H. M.; Reedijk, J. *Biochemistry* **1985**, *24*, 707. Sip, M.; Schwartz, A.; Vovelle, F.; Ptak, M.; Leng, M. *Biochemistry* **1992**, *31*, 2508. Takahara, P. M.; Rosenzweig, A. C.; Frederick, C. A.; Lippard, S. J. *Nature* **1995**, *377*, 649. Takahara, P. M.; Frederick, C. A.; Lippard, S. J. *J. Am. Chem. Soc.* **1996**, *118*, 12309.
(7) Huang, H.; Zhu, L.; Reid, B. R.; Drobny, G. F.; Hopkins, P. B. *Science* **1995**, *270*, 1842. Paquet, F.; Pérez, C.; Leng, M.; Lancelot, G.; Malinge, J.-M. *J. Biomol. Struct. Dyn.* **1996**, *14*, 67.
(8) Reily, M. D.; Marzilli, L. G. *J. Am. Chem. Soc.* **1986**, *108*, 6785. Pt (a recent review contains relevant X-ray structures): Lippert, B. *Prog. Inorg. Chem.* **1989**, *37*, 1. Zn: Miller, S. K.; van der Veer, D. G.; Marzilli, L. G. *J. Am. Chem. Soc.* **1985**, *107*, 1048. Cu: Chiang, C. C.; Sorrell, T.; Kistenmacher, T. J.; Marzilli, L. G. *J. Am. Chem. Soc.* **1978**, *100*, 5102. Co: Poojary, M. D.; Monohar, H. *J. Chem. Soc., Chem. Commun.* **1982**, 533. Cd: Goodgame, D. M. L.; Jeeves, I.; Reynolds, C. D.; Skapski, A. C. *Nucleic Acids Res.* **1975**, *2*, 1375.

S0020-1669(97)00704-0 CCC: $14.00

phosphodiester group, normally only HT complexes are detected in solution and in most solid state crystallographic studies.[8,9] An investigation on complexes of the type $[Pt(5'GMP)_2(RSSR\text{-}Me_2DAB)]^{2-}$ (5′GMP = 5′-guanosine monophosphate; Me_2-DAB = 2,3-bis(methylamino)butane with configurations *R*, *S*, *S*, and *R* at N, C, C, and N, respectively) led to the first evidence for the existence of such an HH atropisomer in solution.[10] In addition, the HH isomer was found to exist in equilibrium with two HT isomers, one HT isomer being predominant. For the complex with all asymmetric centers on Me_2DAB inverted, $[Pt(5'GMP)_2(SRRS\text{-}Me_2DAB)]^{2-}$, the dominant HT isomer had the opposite conformation. A similar investigation of the less symmetrical $[Pt(5'GMP)_2(SRRR\text{-}Me_2DAB)]^{2-}$ and $[Pt(5'GMP)_2(RSSS\text{-}Me_2DAB)]^{2-}$ species with both *N*−Me substituents on the same side of the coordination plane found no clear preference for one HT isomer.[4] These results demonstrated that the stereochemistry of the amine ligand influences the conformational equilibrium between atropisomers.

Preparatory to extending our investigations to DNA and nucleotide adducts of Pt complexes with six-membered chelate rings, we have synthesized and evaluated platinum dichloro and diiodo complexes of 2,4-bis(methylamino)pentane (Me_2DAP), a ligand which has four asymmetric centers when coordinated. These studies allowed us to gain an understanding of the conformations of the coordinated ligands and provided a useful basis for probing the utility of a molecular mechanics/dynamics (MMD) method that employed a force field applicable to nucleic acids.

Experimental Section

Starting Materials. Commercial reagent grade chemicals were used without further purification.

Preparation of the Ligands. The preparation of 2,4-diaminopentane (DAP), the separation of the racemic and meso forms, and resolution of the enantiomers were carried out as described by Bosnich and Harrowfield.[11] The Me_2DAP preparation is described in detail for the *SS*-DAP species (*SS* being the configurations of the two asymmetric carbons). An aqueous solution of DAP·2HCl (3.75 g, 21.4 mmol in 10 mL) was treated with ethyl ether (150 mL) and, with stirring, with excess KOH (0.5 g). The ether solution was drawn away and the aqueous phase extracted twice more with ethyl ether (100 mL each). The ether solution was dried over Na_2SO_4 and then treated, with vigorous stirring, with trifluoroacetic anhydride (7 mL, 50 mmol). A white solid formed immediately. The reaction mixture was left stirring overnight at room temperature. The white solid (the bis(trifluoroacetamide) of DAP) was collected by filtration, washed with water, and dried. Yield: 50%. A yellow solution of this bis(amide) in DMSO (25 mL, containing KOH, 3 g) was treated with an excess of MeI (5 mL, 80 mmol), and the reaction mixture left stirring overnight at room temperature. The DMSO solution was diluted with an equal volume of water (25 mL), and the resultant solution was extracted with *n*-hexane; evaporation under vacuum of the hexane afforded the bis(trifluoroacetamide) of N,N′-dimethylated DAP as a pale yellow oil. The product was hydrolyzed by treatment with methanol (200 mL) and hydrochloric acid (50 mL, 12 N) followed by heating to reflux (70 °C) for 10 h. The yellow waxy solid obtained after the solvent was removed was triturated with absolute ethanol (2 mL) to give a white solid of *N*,*N*′-Me_2DAP·2HCl. This solid was collected by filtration, washed with absolute ethanol, and dried. Yield: 68% (global yield with respect to the unmethylated diamine 35%). Anal. Calcd for $C_7H_{20}Cl_2N_2$: C, 41.4; H, 9.9; N, 13.8. Found for *SS*-Me_2DAP·2HCl: C, 41.2; H, 9.8; N, 13.6. Found for *RR*-Me_2DAP·2HCl: C, 41.2; H, 10.0; N, 13.7. Found for *RS*-Me_2DAP·2HCl: C, 41.5; H, 9.8; N, 13.5. α_D: *SS*-Me_2DAP, −26°; *RR*-Me_2DAP, +26°.

Preparation of the Complexes with Me_2DAP. Two different procedures were used to prepare the complexes.[12,13] The Romeo[13] method is described in detail for the *RR*-Me_2DAP species. A stoichiometric amount of DMSO (112 μL, 1.6 mmol) was added to a water solution of K_2PtCl_4 (327 mg, 0.8 mmol in 10 mL) and the solution kept at 70 °C for 0.5 h; meanwhile the color changed from red to golden yellow (formation of *cis*-$[PtCl_2(DMSO)_2]$). An aqueous solution of *RR*-Me_2DAP·2HCl (150 mg, 0.8 mmol, in 4 mL) was neutralized by addition of $LiOH·H_2O$ (66.1 mg, 1.6 mmol), and the resulting solution was added dropwise to the solution of *cis*-$[PtCl_2(DMSO)_2]$. When the solution became colorless (formation of $[PtCl(DMSO)(Me_2DAP)]Cl$, 15 min), an excess of LiCl (0.5 g) was added and the temperature raised to 95 °C for 3 h. The resulting yellow solution was evaporated to dryness; the residue was extracted with CH_2Cl_2, and the solution was filtered and evaporated to dryness to give pure $[PtCl_2(Me_2DAP)]$. Yield: 85%. Anal. Calcd for $C_7H_{18}Cl_2N_2Pt$: C, 21.2; H, 4.6; N, 7.1. Found for $[PtCl_2(RR\text{-}Me_2DAP)]$: C, 21.1; H, 4.4; N, 7.0. Found for $[PtCl_2(SS\text{-}Me_2DAP)]$: C, 21.4; H, 4.6; N, 6.9. Found for $[PtCl_2(RS\text{-}Me_2DAP)]$: C, 21.2; H, 4.6; N, 7.0.

The Dhara method[12] is described in detail for the *RR*-Me_2DAP species. A solution of K_2PtCl_4 (220 mg, 0.5 mmol, in 10 mL of water) was treated with an excess of KI (4 g) to give (10 min) a brown solution of K_2PtI_4. An aqueous solution of *RR*-Me_2DAP·2HCl (108 mg, 0.5 mmol, in 4 mL) was neutralized by addition of $LiOH·H_2O$ (42 mg, 1 mmol), and the resulting solution was added dropwise to the solution of K_2PtI_4. After 5 min, a dark green precipitate formed. The suspension was left stirring overnight at room temperature; the yellow solid, $[PtI_2(Me_2DAP)]$, that precipitated was washed with water and dried. Yield: 88%. Anal. Calcd for $C_7H_{18}I_2N_2Pt$: C, 14.5; H, 3.1; N, 4.8. Found for $[PtI_2(RR\text{-}Me_2DAP)]$: C, 14.5; H, 3.2; N, 4.8. Found for $[PtI_2(SS\text{-}Me_2DAP)]$: C, 14.5; H, 3.1; N, 4.7. Found for $[PtI_2(RS\text{-}Me_2DAP)]$: C, 14.6; H, 3.0; N, 4.7. The iodo species was converted to the chloro one by treatment of $[PtI_2(Me_2DAP)]$ (290 mg, 0.5 mmol, dissolved in 15 mL of acetone) with $AgNO_3$ (170 mg, 1 mmol, dissolved in 3 mL of water); after 2 h, the colorless solution was filtered and the solvent evaporated. The pale yellow oily residue, $[Pt(NO_3)_2(Me_2DAP)]$, was dissolved in water, and the solution was treated with an excess of KCl; after 15 min of stirring, the water was removed under reduced pressure and the residue ($[PtCl_2(Me_2DAP)]$, KCl, and KNO_3) extracted with CH_2Cl_2. The dichloromethane solution was evaporated to dryness to give pure $[PtCl_2(Me_2DAP)]$. Yield: 73%.

Separation of the Complex Isomers. Isomers were separated by open column gravity silica gel chromatography with CH_2Cl_2 containing from 1 to 15% acetone (v/v) as eluant. $[PtX_2(Me_2DAP)]$ complexes with an enantiomeric form of the ligand (e.g., *RR*-Me_2DAP) have three possible configurations, namely, *SRRR*, *RRRR*, and *SRRS* at N, C, C, and N, respectively. Indeed, three isomers (**A**, **B**, and **C**) were obtained in respective ratios of 9:1:∼0 for the diiodo species and 7:3:1 for the dichloro species. Complexes with the meso ligand (*RS*-Me_2DAP) have four possible configurations, namely, *SRSR*, *RRSS*, *RRSR*, and *SRSS* at N, C, C, and N, respectively (the latter two constitute an enantiomeric pair). Only the first two symmetrical isomers (**D** and **E**) were obtained in the ratios (**D**:**E**) of 9:1 for the diiodo and 1:1 for the dichloro species. ^1H NMR data for the chloro and iodo species for the five isomers (**A**−**E**) are reported in Table 1.

Physical Measurements. IR spectra were recorded as KBr pellets (4000−400 cm^{-1}) or as polythene pellets (400−200 cm^{-1}) on a Perkin-Elmer 283 spectrometer. ^1H NMR spectra were obtained with a Bruker AM 300 spectrometer.

Modeling of Cl Compounds. Previous modeling studies have utilized the AMBER force field, which is commonly used for modeling of DNA and proteins,[14] with modifications to include parameters for platinum and the amine ligands.[15] This force field was further extended

(9) For references to HH species from crystal structures of *cis*-$[Pt(NH_3)_2(9\text{-}EtG)_2]X_2$, see: Lippert, B.; Raudaschl-Sieber, G.; Lock, C. J. L.; Pilon, P. *Inorg. Chim. Acta* **1984**, *93*, 43. Schöllhorn, G.; Raudaschl-Sieber, G.; Müller, G.; Thewalt, U.; Lippert, B. *J. Am. Chem. Soc.* **1985**, *107*, 5932.

(10) Xu, Y.; Natile, G.; Intini, F. P.; Marzilli, L. G. *J. Am. Chem. Soc.* **1990**, *112*, 8177.

(11) Bosnich, B.; Harrowfield, J. MacB. *J. Am. Chem. Soc.* **1972**, *94*, 10.

(12) Dhara, S. C. *Indian J. Chem.* **1970**, *8*, 193.

(13) Romeo, R.; Minniti, D.; Lanza, S.; Tobe, M. L. *Inorg. Chim. Acta* **1977**, *22*, 87.

(14) Weiner, S. J.; Kollman, P. A.; Case, D. A.; Singh, U. C.; Ghio, C.; Alagona, G.; Profeta, S., Jr.; Weiner, P. *J. Am. Chem. Soc.* **1984**, *106*, 765.

(15) Yao, S.; Plastaras, J. P.; Marzilli, L. G. *Inorg. Chem.* **1994**, *33*, 6061.

Table 1. ^{1}H NMR Data (δ, Downfield from $SiMe_4$; $CDCl_3$ Solvent) for $[PtX_2(Me_2DAP)]$ Complexes (X = Cl, I)

complex (ligand config.)		chemical shifts (δ)					^3J coupling constants (Hz)							
		$C^{2,4}Me$	$C^{2,4}H$	NH	NMe	C^3H_2	$C^{2,4}H$, $C^{2,4}Me$	$C^{2,4}H$, C^3H_{ax}	$C^{2,4}H$, C^3H_{eq}	$C^{2,4}H$, NH	C^3H_{ax}, C^3H_{eq}	NH, NMe	$C^{2,4}H$, Pt	NMe, Pt
A^{I} (*SRRR*)	X	1.69	2.90	4.30	2.84	(1.45,	6.5	3.5	<2	<2	16.6	6−6.5	50.2	39.1
	Y	1.21	3.70	4.30	2.67	2.18)	6.5	12.5	<2	<2		6−6.5	*b*	39.1
A^{Cl} (*SRRR*)	X	1.67	2.64	4.46	2.89	(1.38,	6.7	3.4	1.6	2	16.8	6.1	54	34
	Y	1.20	3.71	4.57	2.69	2.10)	6.7	12.1	4	2		6.1	*b*	34
B^{I} (*RRRR*)		1.27	3.84	4.01	2.65	1.85	6.8	9.1		<2	*a*	6.0	*b*	*d*
B^{Cl} (*RRRR*)		1.27	3.94	4.68	2.63	1.83	6.7	9.1		<2	*a*	6.1	*b*	38
C^{Cl} (*SRRS*)		1.42	2.85	3.88	2.92	1.90	6.7	5.8		*c*	*a*	6.4	*e*	33.9
D^{I} (*SRSR*)		1.46	2.80	4.05	2.89	1.80	6.6	12	3	*e*	15.3	6.0	*b*	39
						2.28								
D^{Cl} (*SRSR*)		1.41	2.64	4.15	2.92	1.76	6.5	10	2.8	5.8	16	6.0	*b*	39
						2.22								
E^{I} (*RRSS*)		1.23	3.58	4.35	2.68	1.75	6.7	9.8	1.34	3	16	6.0	*b*	39.5
						1.90								
E^{Cl} (*RRSS*)		1.21	3.61	4.56	2.72	1.39	6.6	11.7	2.01	3.35	15.6	6.0	*b*	39
						1.81								

[a] The two methylene protons are equivalent. [b] This coupling constant is expected to be rather small (*ca*. 15 Hz) and is not observed due to the large multiplet of this proton. [c] The low solubility of this compound precluded obtaining an intense spectrum. [d] **B^{I}** was not completely separated from **A^{I}**, and the *N*−Me and NH couplings with Pt were obscured by signals of **A^{I}** impurity. [e] Obscured by overlapping *N*−Me signal.

to include parameters for chloride coordinated to Pt. Two new potential types, designated IM1 and IM2, were used for the chloride ligands. In this labeling, IM1 is *trans* to N31 and *cis* to N32, where N31 and N32 designations were arbitrarily assigned to the two amine nitrogens.

For a variety of *cis*-$PtCl_2A_2$ complexes, where A_2 represents two unidentate ligands or one didentate amine ligand, a bond length of 2.03 Å and a force constant of 366 kcal/(mol·Å^2) have been used for the Pt−N bond.[15] Typical Pt−Cl bond lengths of *cis*-$PtCl_2A_2$ compounds are ∼2.33 Å,[16−20] and on the basis of the IR spectra of $Pt(NH_3)_4^{2+}$ and $PtCl_4^{2-}$, the Pt−Cl bond is expected to be weaker than the Pt−N bond.[21,22] Therefore, a force constant of 240 kcal/(mol·Å^2) was selected. The right-angle parameters of the *cis* ligand bonds and the coaxial parameters of the *trans* bonds used previously for the modeling of platinum complexes of guanine derivatives[15,23] were adopted here. The van der Waals (vdW) radius (1.92 Å) and ϵ value (0.236) for the chloride ligands were obtained from the values for Cl bonded to carbon.[24]

Atomic charge calculations were performed on *cis*-$[PtCl_2(NH_3)_2]$ by using the Gaussian-92/DFT package.[25] The population analysis for the evaluation of the atomic charges was calculated using the Hartree−Fock method[26] and the LANL2DZ basis set.[25] An idealized geometry was used for the *cis*-$[PtCl_2(NH_3)_2]$ molecule (distances (Å) Pt−N 2.05, Pt−Cl 2.33, N−H 1.02; angles of 90 and 180° for the coordination sphere and 110° for Pt−N−H and H−N−H). The atomic charges found were as follows: Pt, 0.334; Cl, −0.322; N, −1.077; H, 0.411. The Pt and Cl charges were used for the $[PtCl_2(Me_2DAP)]$ MMD calculations. Charges on the Me_2DAP ligand were modified from the starting values obtained within the CFF91 force field; the additional 0.310 unit of charge necessary to make the $[PtCl_2(Me_2DAP)]$ compound neutral was distributed to the atoms in the Me_2DAP ligand on the basis of their proximity to the platinum as described previously (Table 2).[15] It was found that the charges on the atoms did not have a significant influence on the final energies of the conformations.

Table 2. Atomic Charges Used for Molecular Mechanics Calculations[a]

atom	unplatinated charge	platinated charge	atom	unplatinated charge	platinated charge
$N^{2,4}$	−0.414	−0.350	$C^{1,5}$	−0.159	−0.153
H(N)	+0.249	+0.268	C^3	−0.106	−0.094
$C^{6,7}$	−0.076	−0.057	$H(C^{1,5})$, $H(C^3)$	+0.053	+0.053
$H(C^{6,7})$	+0.053	+0.059	Pt	N/A	+0.334
$C^{2,4}$	+0.030	+0.049	Cl	N/A	−0.322
$H(C^{2,4})$	+0.053	+0.059			

[a] See Figure 2 for atom-labeling schemes.

MMD calculations were performed on a Silicon Graphics INDY R5000 workstation using InsightII version 95.0 from Biosym Inc. Dynamics calculations were used to simulate heating of the structures to 1800 K for 500 ps (heating to 1800 K was necessary to overcome the conformational energy barriers on the picosecond time scale), and the structure was saved after each picosecond. After 500 different structures were generated, they were subjected to steepest descent minimization for 100 iterations followed by conjugate gradient minimization for 5000 iterations or until the maximum rms derivative was less than 0.001 kcal/(mol·Å). Calculated energies for the different conformations of isomers **A**−**E** are reported in Table 3.

X-ray Crystallography. Well-formed parallelepipeds of the chloro (**D^{Cl}**, colorless) and iodo (**D^{I}**, yellow) **D** isomer were mounted on glass fibers for the X-ray data collections on a Siemens P4 diffractometer (crystallographic details in Table 4). Unit cell parameters were computed by least-squares refinement of the values of 30 carefully centered and randomly selected reflections (2θ, 10−40°). Intensities were corrected for Lorentz, polarization, and absorption effects (ψ scan technique based on four reflections).

The structure solutions and refinements were performed by Patterson and Fourier methods. The Fourier difference of **D^{Cl}** clearly showed all the H atoms which were included in the last cycles of refinement and refined freely. All the H atoms of **D^{I}** were set in calculated positions. All the heavy atoms were treated anisotropically, whereas all the H atoms were refined isotropically. The thermal parameters for the H atoms of **D^{Cl}** were refined freely for $N^{2,4}H$ and constrained to 0.06, 0.08, and 0.07 Å^2 for $C^{1,5}H_3$, $C^{2,4}H$, and C^3H_2, respectively. The thermal parameters for the H atoms of **D^{I}** were constrained to 1.5 times the value of the U_{eq} of the atoms to which they are bound. The full-matrix least-squares cycles converged to R_1 and wR_2 of 0.0266 and

(16) Arpalahti, J.; Lippert, B.; Schollhorn, H.; Thewalt, U. *Inorg. Chim. Acta* **1988**, *153*, 45.
(17) Wimmer, S.; Wimmer, F.; Jaud, J.; Johnson, N. P.; Castan, P. *Inorg. Chim. Acta* **1988**, *144*, 25.
(18) Lock, C. J. L.; Pilon, P. *Acta Crystallogr.* **1981**, *B37*, 45.
(19) Lock, C. J. L.; Zvagulis, M. *Inorg. Chem.* **1981**, *20*, 1817.
(20) Milburn, G. H. W.; Truter, M. R. *J. Chem. Soc.* **1966**, 1609.
(21) Mizushima, S.-I.; Nakagawa, I.; Schmelz, M. J.; Curran, C.; Quagliano, J. V. *Spectrochim. Acta* **1958**, *13*, 31.
(22) Goggin, P. L.; Mink, J. *J. Chem. Soc., Dalton Trans.* **1974**, 1479.
(23) Kozelka, J.; Archer, S.; Petsko, G. A.; Lippard, S. J.; Quigley, G. J. *Biopolymers* **1987**, *26*, 1245.
(24) Allinger, N. L.; Hirsch, J. A.; Miller, M. A.; Tyminski, I. J. *J. Am. Chem. Soc.* **1969**, *91*, 337.
(25) Frisch, M. J.; Trucks, G. W.; Head-Gordon, M.; Gill, P. M. W.; Wong, M. W.; Foresman, J. B.; Johnson, B. G.; Schlegel, H. B.; Robb, M. A.; Reploge, E. S.; Gomperts, R.; Andres, J. L.; Raghavachari, K.; Binkley, J. S.; Gonzales, C.; Martin, R. L.; Fox, D. J.; Defrees, D. J.; Baker, J.; Stewart, J.-J. P.; Pople, J. A. *GAUSSIAN 92*; Gaussian Inc.: Pittsburgh, PA, 1992.
(26) Hehre, W. J.; Radom, L.; Schleyer, P. v. R.; Pople, J. A. *Ab Initio Molecular Orbital Theory*; Wiley: New York, 1986.
(27) Sheldrick, G. M. SHELX 86, program for the solution of crystal structures, University of Göttingen, Germany, 1986.

Table 3. Calculated Energies for $[PtCl_2(Me_2DAP)]$ Compounds

isomer	confign	energy (kcal)	conformn of six-membered ring
A	*SRRR*	8.36[a]	δ-chair
		12.13	λ-skew
		12.52	distorted λ-boat
		12.77	λ-chair
		16.31	λ-boat
		17.19	δ-boat
B	*RRRR*	8.22[a]	λ-skew
		9.47	chair[b]
		16.63	δ-skew
C	*SRRS*	10.20[a]	chair[b]
		11.86	distorted boat[b]
		15.00	δ-skew
D	*SRSR*	11.12	δ-chair
		11.91	distorted λ-boat
		12.29	λ-chair
		13.77[a]	skew[b]
		14.73	λ-boat
		21.99	half chair
E	*RRSS*	6.99[a]	λ-chair
		12.65	skew[b]
		14.43	δ-chair
		18.04	λ-boat

[a] Conformation determined by NMR spectroscopy. [b] Structures in which λ and δ are equivalent.

Table 4. Crystal Data and Structure Refinement Details for $\mathbf{D^{Cl}}$ and $\mathbf{D^{I}}$ [a]

	$\mathbf{D^{Cl}}$	$\mathbf{D^{I}}$
empirical formula	$C_7H_{18}Cl_2N_2Pt$	$C_7H_{18}I_2N_2Pt$
fw	396.2	579.1
space group	*Pnma*	$P2_1/n$
unit cell dimens		
a (Å)	11.9980(10)	8.408(4)
b (Å)	13.167(2)	15.774(4)
c (Å)	7.4490(8)	10.190(4)
β (deg)	90	102.17(3)
V (Å^3)	1176.8(2)	1321.1(9)
Z	4	4
D_{calcd} (Mg m^{-3})	2.236	2.918
abs coeff (mm^{-1})	12.33	15.32
no. of reflns collected	2164	4830
no. of data, restraints, params	1082, 0, 87	2280, 0, 109
goodness-of-fit on F^2	1.075	1.026
Final R indices ($I > 2\sigma_I$)	$R_1 = 0.0266$, w$R_2 = 0.0594$	$R_1 = 0.0559$, wR_2=0.1287
R indices (all data)	$R_1 = 0.0343$, w$R_2 = 0.0626$	$R_1 = 0.0830$, w$R_2 = 0.1445$
Largest diff peak and hole (e Å^{-3})	1.346 and −1.796	4.524 and −1.905

[a] For all structures Mo Kα radiation was used at $T = 293(2)$ K. $R_1 = \Sigma||F_o| - |F_c||/\Sigma|F_o|$; w$R_2 = [\Sigma w(F_o^2 - F_c^2)^2/\Sigma w(F_o^2)^2]^{1/2}$. Refinement method: full-matrix least-squares on F^2.

0.0594 for $\mathbf{D^{Cl}}$ and to 0.0559 and 0.1287 for $\mathbf{D^{I}}$. The calculations, on Pentium Olidata and on VAX 6610 computers, utilized SHELX 86,[27] SHELX 93,[28] and PARST 95 (analysis of the geometry)[29] packages. Selected bond distances and angles are listed in Table 5; atomic coordinates for the structures are given in Tables S2 ($\mathbf{D^{Cl}}$) and S3 ($\mathbf{D^{I}}$) (Supporting Information).

Results

Ligand Synthesis. The chiral diamine was resolved prior to methylation at nitrogen atoms, since procedures for this resolution were well established. This synthetic strategy required a method which afforded a product with exactly one methyl substituent on each nitrogen atom. Reactions of diamines with alkylating compounds such as alkyl halides produce a mixture of alkylated products from which it is difficult, if not impossible, to isolate the acceptably pure N,N′-dialkylated product. Therefore we developed a facile route to produce an N,N′-disubstituted diamine in high purity and with acceptable yield. This route involved formation of the bis-(trifluoroacetamide) from the parent diamine followed by methylation of the diamide with MeI under basic conditions and hydrolysis of the *N*−Me amide under acidic conditions.

Synthesis of the Complexes. Two different synthetic procedures were used for the platinum complexes. (I) The procedure of Dhara, consisting of two steps: synthesis of the diiodo complex by reaction of $[PtI_4]^{2-}$ with the diamine and the conversion of the diiodo species into the dichloro complex.[12] (II) The procedure of Romeo *et al.*, which consists of the preparation of *cis*-$[PtCl_2(DMSO)_2]$ by reaction of $[PtCl_4]^{2-}$ with DMSO (molar ratio 1:2), followed by displacement of the DMSO ligands by the diamine.[13] The two procedures gave a different ratio of isomers separable by chromatography.

Complexes Formed from *RR*-Me_2DAP. We confine the description to $[PtX_2(RR\text{-}Me_2DAP)]$ compounds, since the $[PtX_2(SS\text{-}Me_2DAP)]$ compounds gave identical spectra, as expected since X is not chiral. For $[PtX_2(RR\text{-}Me_2DAP)]$ complexes, *R* and *S* chiralities are possible at each N atom; thus, three configurational isomers (configurations *SRRR*, *RRRR*, and *SRRS* at the N, C, C, and N asymmetric centers, respectively) are possible. These are shown in Chart 1, where we also indicate the ligand conformations (chair, skew, and boat) and ring puckers (λ and δ). Because the three ring carbons (C^2−C^4) and the metal center are coplanar, there is a true helicity of the ring pucker for the skew conformation. In this case, helicity is defined as λ and δ if moving along C^2−C^4 as indicated by the index finger, the advancement along the axis connecting the two nitrogens is in the direction indicated by the thumb of the left and right hands, respectively. However, for the boat and chair conformations, the metal atom is out of the plane of the C^2−C^4 moiety and there is no true helicity. Therefore, we specify the ring puckers by choosing one carbon bond of the bridging chain (namely C^2−C^3) to define a pseudohelicity (λ and δ, according to the rules given above) for these two cases.

Three isomers (**A**, **B**, and **C**) were obtained as expected. One isomer (**A**) proved to be unsymmetrical (two resonances for each type of ligand proton), and the other two (**B** and **C**) proved to be symmetrical (one resonance for each type of ligand proton) (Figure 1). Therefore, isomer **A** must have the *SRRR* configuration, and isomers **B** and **C** must have the *RRRR* and *SRRS* configurations.

First, we assign the two sets of NMR signals (X and Y, differentiated easily on the basis of H,H couplings) to the *SR* and *RR* halves of the ligand in the *SRRR* isomer (**A**). The three-bond coupling ($^3J_{Pt,H}$) between the Pt and the H atoms on the asymmetric carbons ($C^{2,4}$) is ∼54 Hz in set X but less than 15 Hz in set Y. This major difference may be due to the Karplus type angular dependence of $^3J_{Pt,H}$.[30] Chart 2 shows a chelate ring viewed down one of the N−C bonds in the chair and skew conformations (a) and in the boat conformation (b). $^3J_{Pt,H_{eq}}$ should be greater than $^3J_{Pt,H_{ax}}$, since Φ_{eq} is ∼180° and Φ_{ax} is ∼60°. Therefore set X belongs to the half of the *SRRR*-Me_2-DAP ligand having an essentially equatorial $C^{2,4}$H, and set Y belongs to a half-ligand having an essentially axial $C^{2,4}$H. The

(28) Sheldrick, G. M. SHELX 93, program for the refinement of crystal structures. University of Göttingen, Germany, 1993.
(29) Nardelli, M. PARST 95, a system of computer routines for calculating molecular parameters from the results of crystal structure analysis. University of Parma, Italy, 1995.
(30) Erickson, L. E.; McDonald, J. W.; Howie, J. K.; Clow, R. P. *J. Am. Chem. Soc.* **1968**, *90*, 6371.

Table 5. Bond Lengths (Å) and Angles (deg) for $\mathbf{D^{Cl}}$ and $\mathbf{D^{I}}$

lengths				angles					
$\mathbf{D^{Cl}}$		$\mathbf{D^{I}}$		$\mathbf{D^{Cl}}$		$\mathbf{D^{I}}$			
Pt−Cl^1	2.314(2)	Pt−I^1	2.5859(14)	Cl^1−Pt−Cl^2 [a]	93.98(9)	I^1−Pt−I^2	93.20(5)		
		Pt−I^2	2.5887(14)	N^2−Pt−Cl^1	86.1(2)	N^2−Pt−I^1	87.2(4)	N^4−Pt−I^2	88.2(4)
Pt−N^2	2.057(5)	Pt−N^2	2.057(13)	N^2−Pt−Cl^2 [a]	179.8(1)	N^2−Pt−I^2	177.9(4)	N^4−Pt−I^1	178.5(4)
		Pt−N^4	2.088(12)	N^2−Pt−N^4 [a]	93.8(3)	N^2−Pt−N^4	91.3(6)		
N^2−C^2	1.477(8)	N^2−C^2	1.48(2)	Pt−N^2−C^2	115.1(4)	Pt−N^2−C^2	118.0(10)	Pt−N^4−C^4	114.5(10)
		N^4−C^4	1.48(2)	Pt−N^2−C^6	111.7(4)	Pt−N^2−C^6	112.6(11)	Pt−N^4−C^7	112.1(11)
N^2−C^6	1.501(9)	N^2−C^6	1.47(2)	C^2−N^2−C^6	113.5(5)	C^2−N^2−C^6	112.3(14)	C^4−N^4−C^7	113(2)
		N^4−C^7	1.50(2)	N^2−C^2−C^1	108.5(6)	N^2−C^2−C^1	108.7(14)	N^4−C^4−C^5	107(2)
C^1−C^2	1.510(10)	C^1−C^2	1.55(3)	N^2−C^2−C^3	112.8(6)	N^2−C^2−C^3	112.2(13)	N^4−C^4−C^3	114(2)
		C^4−C^5	1.52(3)	C^1−C^2−C^3	116.1(7)	C^1−C^2−C^3	114.6(13)	C^5−C^4−C^3	118(2)
C^2−C^3	1.527(7)	C^2−C^3	1.52(2)	C^2−C^3−C^4[a]	120.8(8)	C^2−C^3−C^4	120.6(14)		
		C^3−C^4	1.49(2)						

[a] In $\mathbf{D^{Cl}}$ the C^4, C^5, C^7, Cl^2, and N^4 atoms are related to C^2, C^1, C^6, Cl^1, and N^2 atoms, respectively, by the symmmetry transformation $x, -y + {}^1/_2, z$.

Chart 1. Schematic Drawing of the Possible Configurations and Conformations for [PtX_2(*RR*-Me_2DAP)]

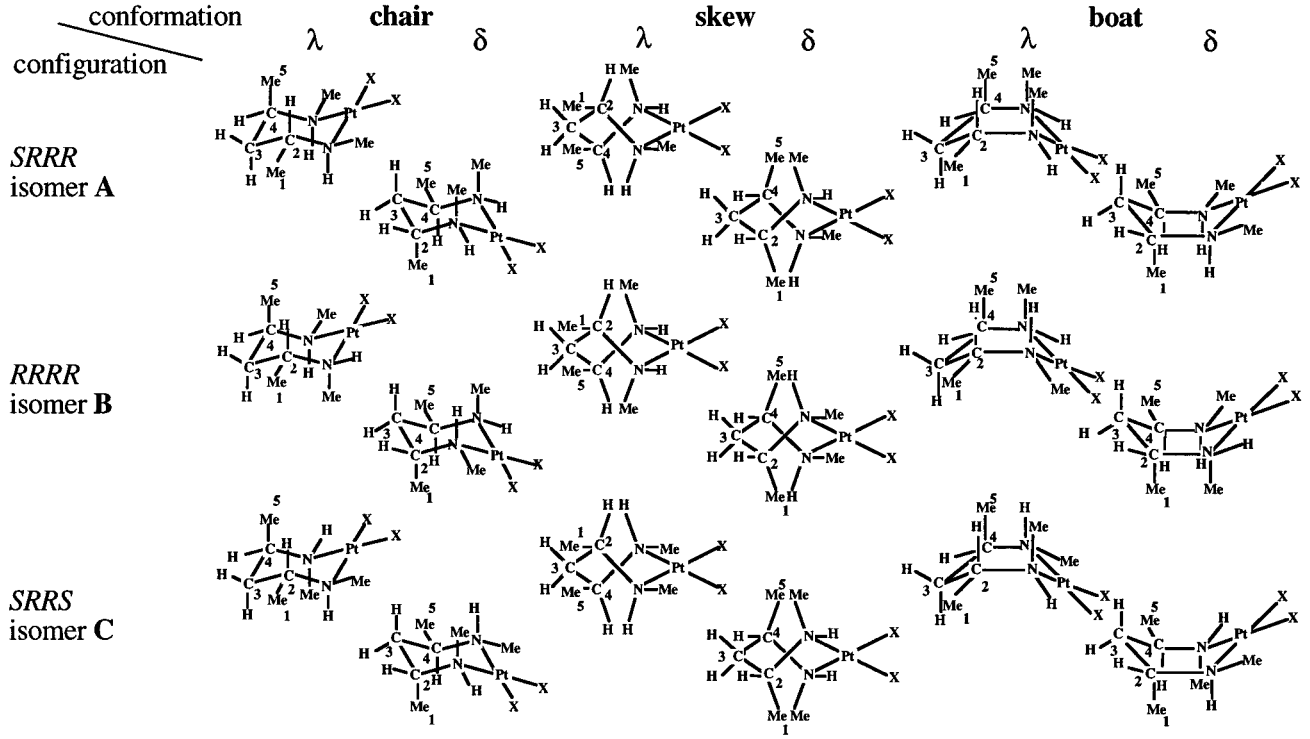

difference in $^3J_{Pt,H}$ values for the halves of the ligand rules out both of the following conformations: skew [since these have equivalent C^{2,4}H's, either both axial (λ-skew) or both equatorial (δ-skew)] and boat [since both C^{2,4}H's are related to Pt by a torsion angle of 120°]. Furthermore, if the two chair conformations (λ and δ) are equally postulated, each C^{2,4}H will spend equal time as an axial and as an equatorial proton. Then both observed $^3J_{Pt,H}$ would be the average of $^3J_{Pt,H_{ax}}$ and $^3J_{Pt,H_{eq}}$; but, this is not the case. Therefore we conclude that only one of the two chair conformations (either λ or δ) is favored.

Further NMR evidence in support of the conclusion that one chair conformation dominates comes from the two multiplets centered at δ 1.38 and 2.10 for the central C^{3}H$_2$ protons. The values of $^3J_{H,H}$ are all $\leq$3−4 Hz except for that between the C^{3}H at δ 2.10 and the C^{2,4}H at δ 3.71 (set Y with the C^{2,4}H essentially axial, 12 Hz). Since only the $J_{H_{ax},H_{ax}}$ is expected to be large while both the $J_{H_{ax},H_{eq}}$ and $J_{H_{eq},H_{eq}}$ are expected to be small, we can conclude that C^{3}H at δ 2.10 is also essentially axial and the other C^{3}H at δ 1.38 essentially equatorial, therefore confirming that the molecule remains essentially in one of the two chair conformations. In order to decide which of the two chair conformers is preferred, it is worth examining the $^3J_{H,H}$ between adjacent C^{2,4}H and NH. In both sets, these coupling constants are very small (*ca.* 2 Hz). In the δ-chair conformation, both NH's are in equatorial positions and a small coupling is expected regardless of the equatorial or axial position of the adjacent C^{2,4}H (J_{60}).[31] For the λ-chair conformation, large (set Y) and small (set X) coupling constants between adjacent C^{2,4}H and NH would be expected. Therefore the small coupling constants are in accord with δ-chair conformation. Further support to the bis-axial disposition of the *N*-Me's came from a NOE experiment showing that the cross peak between *N*-Me's is far more intense than those between N−Me and *C*-Me groups (the opposite trend would be expected if the preferred conformation was λ). From the conclusion that the δ-chair conformation is favored, it follows that set X belongs to the *SR* half and set Y to the *RR* half of the *SRRR*-Me_2DAP ligand.

In addition to coupling constants, sets X and Y of isomer **A** have significant differences in chemical shifts, particularly the

(31) J_0, J_{60}, J_{120}, and J_{180} designate the coupling constant between two protons separated by torsion angles of 0, 60, 120, and 180°, respectively.

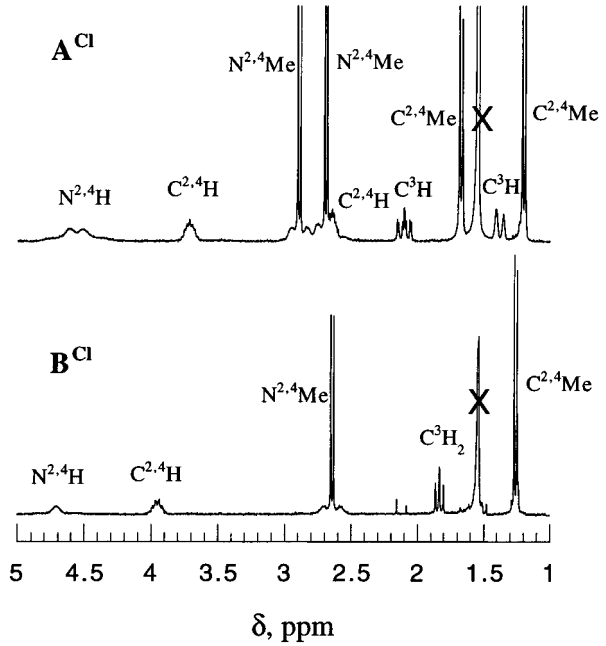

Figure 1. ^{1}H NMR spectra of [$PtCl_2$(*SRRR*-Me_2DAP)] (**A**^{Cl}) and [$PtCl_2$(*RRRR*-Me_2DAP)] (**B**^{Cl}) (δ, downfield from $SiMe_4$; $CDCl_3$ solvent). The X indicates the water peak.

Chart 2. Portion of the Chelate Ring Viewed down a N−$C^{2,4}$ Bond in the Chair and Skew Conformations (a) and in the Boat Conformation (b)

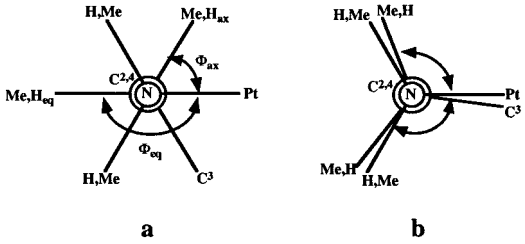

$C^{2,4}$H (∼1 ppm) and $C^{2,4}$Me (∼0.5 ppm) signals. As a consequence, in set X (for the *SR* half) the $\Delta\delta$ between the $C^{2,4}$H (δ 2.65) and $C^{2,4}$Me (δ 1.70) is only 0.95 ppm while in set Y (for the *RR* half) the $\Delta\delta$ between the $C^{2,4}$H (δ 3.70) and $C^{2,4}$Me (δ 1.20) is much larger, 2.50 ppm. The distinct chemical shift patterns permit the straightforward structural assignment of the isomers with a symmetrical ligand. The possible configurations for **B** and **C** are *RRRR* and *SRRS*. In *RRRR*, the adjacent C and N atoms have equal configurations, and therefore a set of shifts similar to Y would be expected; in *SRRS*, the adjacent C and N atoms have opposite configurations, and therefore the shifts should resemble X. Exactly this pattern was observed, so we can confidently assign configuration *RRRR* to isomer **B** and configuration *SRRS* to isomer **C**.

The actual conformation of isomers **B** and **C** could be deduced from the values of $^3J_{H,H}$ between $C^{2,4}$H and C^3H_2. These values are 9.1 and 5.8 Hz for isomers **B** and **C**, respectively. Values of $^3J_{H,H}$ expected for different conformers follow: $0.25\cdot(J_{180} + 3J_{60})$[31] for chair and boat conformations,[32] $0.5(J_{180} + J_{60})$ for λ-skew, and J_{60} for δ-skew conformations.[33] The experimental values are in accord with a predominant contribution of the λ-skew conformation in isomer **B** and a fluxional chair or a fluxional boat conformation in isomer **C**. The observed difference between isomers **B** and **C** [$\Delta(^3J_{H,H}) = 3.3$ Hz] agrees with the difference estimated between λ-skew and chair or boat conformations [$0.25(J_{180} - J_{60})$] from a reasonable value of 12 Hz for $(J_{180} - J_{60})$.

The close similarity between the resonances of isomers **B** and set Y of isomer **A** and between the resonances of isomer **C** and set X of isomer **A** is rather surprising since isomer **A** adopts preferentially a δ-chair conformation while **B** and **C** have either a λ-skew conformation or a fluxional chair conformation. Evidently, the conformation is not the factor primarily influencing the dependence of shift on the relative configuration of the adjacent C and N chiral centers.

Complexes Formed from *RS*-Me_2DAP. Four configurations (*SRSR*, *RRSS*, *RRSR*, and *SRSS*) are possible for the meso ligand in [PtX_2(*RS*-Me_2DAP)]. These are shown in Chart 3, along with all possible conformations. However, only two isomers (**D** and **E**) were formed and both had one resonance for each type of ligand proton. Therefore these isomers must have *SRSR* and *RRSS* configurations. We can assign the configuration by analyzing the chemical shift patterns of the $C^{2,4}$H and $C^{2,4}$Me signals as follows: isomer **D**, with $\delta(C^{2,4}H) - \delta(C^{2,4}Me) = 1.23$ ppm, has opposite configurations on adjacent C and N atoms and therefore has an *SRSR* ligand; and isomer **E**, with $\delta(C^{2,4}H) - \delta(C^{2,4}Me) = 2.40$ ppm, has equal configurations on adjacent C and N atoms and therefore has an *RRSS* ligand.

For both isomers (**D** and **E**), the two chair and the two boat conformations (λ and δ) have symmetrical ligands but different energies; in contrast, skew conformations (λ and δ) have unsymmetrical ligands but equal energy. In each isomer (**D** and **E**), the signals of the central methylene protons (C^3H_2) have very different shifts and multiplicities. In particular, the signal at higher field shows a large geminal coupling (*ca.* 16 Hz) and only a small vicinal coupling (<3 Hz) with the protons of the adjacent asymmetric carbons ($C^{2,4}$H). In contrast, the signal at lower field, in addition to the large geminal coupling, also has a large vicinal coupling with the $C^{2,4}$H signal (*ca.* 10 and 12 Hz for isomers **D** and **E**, respectively). These data exclude δ-chair and δ-boat conformations, since both have the protons of the two asymmetric carbons (C^2 and C^4) in equatorial positions making torsion angles of 60° with the methylene protons. Consequently, both the resulting $^3J_{H,H}$ couplings should be small. The remaining conformations (λ-chair, λ-boat, and fluxional skew) all allow two distinct vicinal couplings ($^3J_{C^3H,C^{2,4}H}$): one small (J_{60}) and one large [J_{180} for λ-chair and λ-boat, $0.5(J_{180} + J_{60})$ for fluxional skew]. The experimental values of the large vicinal coupling (10 and 12 Hz for **D** and **E**, respectively) indicate that the conformation might be fluxional skew for **D** and λ-chair or λ-boat for **E**. Also, the value of coupling constants between adjacent $C^{2,4}$H and NH protons is in accord with **D** (5.8 Hz) having a skew conformation [expected values: $0.5(J_{180} + J_{60})$ for skew, J_{180} for λ-chair, and J_{120} for λ-boat conformation] and with **E** (3.3 Hz) having a λ-chair conformation [expected values: J_{60} for λ-chair and for skew and J_0 for λ-boat conformation].

The effect of temperature on the NMR spectra could also help to distinguish between skew and chair or boat conformations. In the case of the skew conformation, the presence of only one set of signals requires the fast interconversion between the two equivalent conformers (δ and λ) and a lowering of the temperature should cause a broadening of the signals. In contrast, such a broadening would not be observed in the case of a λ-chair or λ-boat conformation having a symmetrical ligand.

(32) Since these two types of conformers exist as equivalent and equally abundant conformers differing only in ring puckering and since within each conformer the ligand is unsymmetrical, the presence of only one set of ^{1}H NMR signals requires a fast conformational interchange.

(33) The two skew conformations related by ring-pucker inversion are inequivalent, and the one having lower energy will be preferred; in this case the presence of only one set of ^{1}H NMR signals stems from the C_2 symmetry of the ligand within each conformer.

Chart 3. Schematic Drawing of the Possible Configurations and Conformations for [PtX_2(*RS*-Me_2DAP)]

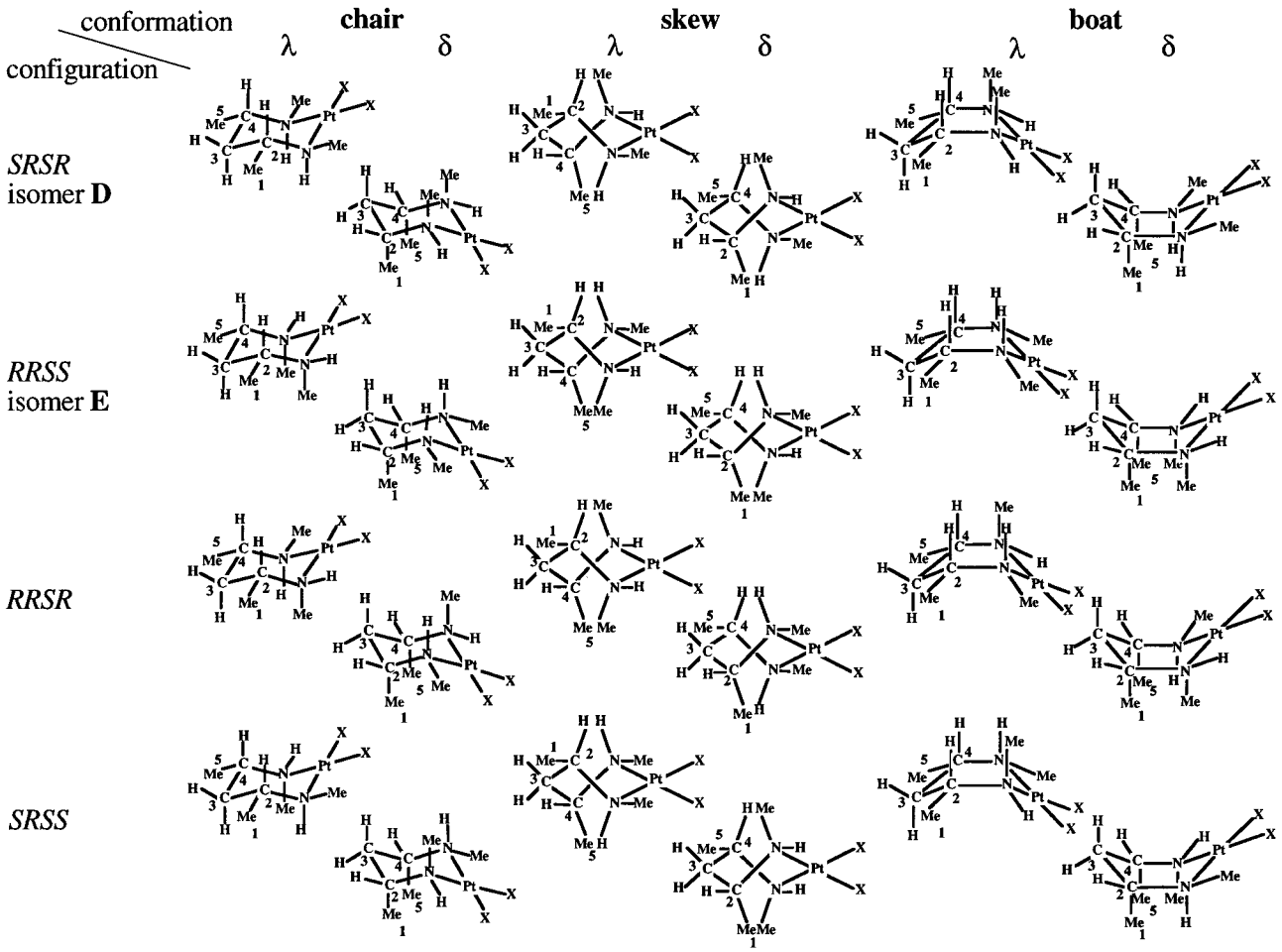

The ^{1}H NMR spectrum of isomer **D** (CD_2Cl_2 solution) starts broadening at −50 °C. The broadening reaches its maximum at *ca.* −75 °C. This behavior rules out a net preference for either the λ-chair or the λ-boat conformation at room temperature (since this would not explain the broadening of the NMR signals on lowering the temperature) and supports a skew conformation although at the lowest temperature the interconversion of the two skew conformers is still rather fast. In contrast, the near absence of a change in the ^{1}H NMR spectrum of isomer **E** (CD_2Cl_2 solution) upon lowering the temperature to −80 °C is in accord with either a λ-chair or a λ-boat conformation.

Modeling of Cl Compounds. In past studies of related Pt complexes, the preferred conformers suggested were different.[34,35] Because of these differences, we used MMD calculations to gain further insight into the preferred solution state conformations for [$PtCl_2$(Me_2DAP)] complexes.

For the majority of the [$PtCl_2$(Me_2DAP)] configurations studied, our calculations suggested that the chair conformations had the lowest energy (Table 3). Isomers **A** and **E** were calculated to prefer the δ- and λ-chair conformations, respectively. Isomer **C** was found to prefer the equivalent chair conformations. However, for isomer **B**, the λ-skew conformation with the *C*-Me's in the equatorial positions and the *N*-Me's in the axial positions appeared to be preferred. These calculated structures agree with those determined experimentally.

Isomer **D** was calculated to prefer the δ-chair conformation, with an energy of 11.1 kcal/mol. Other low-energy conformations were a slightly distorted λ-boat structure (11.9 kcal/mol), the λ-chair conformation (12.3 kcal/mol), and the skew conformations (13.8 kcal/mol). The λ-boat structure was found to have an energy of 14.7 kcal/mol. The energy of the half-chair conformations, which are the intermediates for the chair to skew conformational changes, was found to be 22.0 kcal/mol. The NMR spectra suggest that the skew conformations are actually the lowest in energy.

X-ray Crystal Structure of D^{Cl} and D^{I} Complexes. Because of the apparent conflict between the NMR data and the results of calculations for isomer **D**, we performed an X-ray crystal structure investigation of isomer **D** with chloride ($\mathbf{D^{Cl}}$) and iodide ligands ($\mathbf{D^{I}}$). Molecular structures and atom-labeling schemes are reported in Figures 2 and 3. Selected bond lengths and bond angles are listed in Table 5. The coordination sphere of both complexes has the usual square planar geometry. In $\mathbf{D^{Cl}}$, Pt sits on a mirror plane which passes through C^3 and both the H atoms linked to C^3. The deviation of Pt from the coordination plane is negligible for both the compounds [0.0001(3) Å, $\mathbf{D^{Cl}}$; 0.0195(7) Å, $\mathbf{D^{I}}$]. The Pt−ligating atom distances are in agreement with previous studies.[34,36−40] The Me_2DAP ligand has the *RSRS* configuration, fully consistent with the NMR analysis; however, the conformation (δ-chair for both

(34) Vickery, K.; Bonin, A. M.; Fenton, R. R.; O'Mara, S.; Russell, P. J.; Webster, L. K.; Hambley, T. W. *J. Med. Chem.* **1993**, *36*, 3663.
(35) Sarneski, J. E.; Erickson, L. E.; Reilley, C. N. *Inorg. Chem.* **1981**, *20*, 2137.
(36) Cini, R.; Fanizzi, F. P.; Intini, F. P.; Maresca, L.; Natile, G. *J. Am. Chem. Soc.* **1993**, *115*, 5123.
(37) Oksanen, A.; Kivekäs, R.; Lumme, P.; Laitalainen, T. *Acta Crystallogr.* **1991**, *C47*, 719.
(38) Connick, W. B.; Gray, H. B. *Acta Crystallogr.* **1994**, *C50*, 1040.
(39) Fanizzi, P. F.; Natile, G.; Lanfranchi, M.; Tiripicchio, A.; Clark, R. J. H.; Michael, D. J. *J. Chem. Soc., Dalton Trans.* **1989**, 1689.
(40) Oksanen, A.; Kivekäs, R.; Lumme, P.; Laitalainen, T. *Acta Crystallogr.* **1989**, *C45*, 1493.

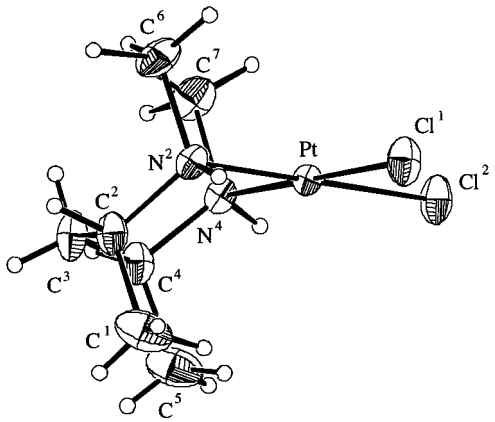

Figure 2. Perspective view of [$PtCl_2$(*SRSR*-Me_2DAP)] ($\mathbf{D^{Cl}}$). Ellipsoids enclose 30% probability. The labeling is shown for all the non-hydrogen atoms even though a crystallographic mirror plane passes through Pt, C^3, and both the H atoms linked to C^3.

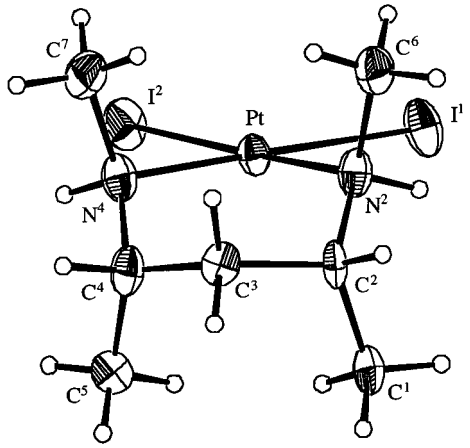

Figure 3. Perspective view of [PtI_2(*SRSR*-Me_2DAP)] ($\mathbf{D^{I}}$). Ellipsoids enclose 30% probability.

compounds) is different from the fluxional skew form deduced from NMR data in solution at room temperature.

It is noteworthy that the δ-chair conformation brings not only the *N*-Me's but also the *C*-Me's in proximity to the Pt atom. The H···Pt contact distances are 2.99(1), and 3.15(1) Å ($\mathbf{D^{Cl}}$) and 2.97(1) and 3.13(1) Å ($\mathbf{D^{I}}$) for N−Me and *C*-Me, respectively (we recall that the H atoms for $\mathbf{D^{I}}$ were set in calculated positions). The sum of the vdW radii for H and Pt is 2.9−3.3 Å.[41] So, one cannot exclude the possibility that the solid state structure is stabilized by attractive interactions between the metal center and the methyl groups. These conclusions seem to be consistent with the different values of the bond angles centered on $C^{2,4}$ and $N^{2,4}$. The Me−$C^{2,4}$−N angles [108.5(6)° ($\mathbf{D^{Cl}}$) and 108(2)° (average) ($\mathbf{D^{I}}$)] are small compared with the other angles centered on $C^{2,4}$ [112.8(6) and 116.1(7)° ($\mathbf{D^{Cl}}$) and 113(2)° (average) and 116(2)° (average) ($\mathbf{D^{I}}$) for $N^{2,4}$−$C^{2,4}$−C^3 and Me−$C^{2,4}$−C^3, respectively]. Similarly the Me−$N^{2,4}$−Pt angles [111.7(4)° ($\mathbf{D^{Cl}}$) and 112(1)° (average) ($\mathbf{D^{I}}$)] are small compared with the other angles centered on $N^{2,4}$ [113.5(5) and 115.1(4)° ($\mathbf{D^{Cl}}$) and 113(2)° (average) and 116(2)° (average) ($\mathbf{D^{I}}$) for Me−$N^{2,4}$−$C^{2,4}$ and Pt−$N^{2,4}$−$C^{2,4}$, respectively].

An intramolecular (Pt)X···H(N) interaction occurs in $\mathbf{D^{Cl}}$ [Cl···N, 2.991(5) Å; Cl···H−N, 108(4)°] and in $\mathbf{D^{I}}$ [I···N, 3.25-(1) Å (average); I···H−N, 110(2)°]. The analysis of the packing also shows that the halogen atoms and the NH groups are connected via a network of H bonds [Cl···N($-x$, $1 - y$, $-z$), 3.423(5) Å; Cl···H−N, 137(5)° ($\mathbf{D^{Cl}}$). N(1)···I(2)($0.5 + x$, $0.5 - y$, $-0.5 + z$), 3.87(1) Å; N(1)−H···I(2), 126(1)° ($\mathbf{D^{I}}$)].

(41) Bondi, A. *J. Phys.Chem.* **1964**, *68*, 441.

Discussion

Saturated five-membered N−C−C−N−M chelate rings are puckered and can assume either the λ or δ conformation. However, if the two carbons of the chelates are asymmetric such as in DACH or DAB (DAB = 2,3-diaminobutane), intraligand steric interactions make the *RR* and *SS* isomers favor the λ and δ conformations, respectively. Finally, neither conformation is favored by the *RS* isomer, which behaves in the same manner as ligands lacking asymmetric centers. In this case, the net situation is that of a planar chelate ring with the ring substituents equally displaced above and below the coordination plane.[4]

In general, compared to these five-membered chelate rings, six-membered rings are more flexible and can adopt chair, skew, and boat conformations. Each conformation can allow two ring puckers: λ and δ (for chair and boat conformations ring substituents are required in order to have distinct ring puckers). NMR results[42] and calculated conformational energies for unsubstituted six-membered chelate rings[34,43] have indicated that the chair conformation is most stable.

Investigations of substituted six-membered chelate rings (e.g., meso and racemic [$PtCl_2$(1,3-diphenyl-1,3-diaminopropane)][44] and the 3-hydroxyphenyl analog[45]) led to the chair conformation with equatorial arrangement of the phenyl rings being favored in the meso form of the complex and interconverting chair conformations with equatorial/axial phenyl rings (with the intermediacy of a favored skew conformation with both phenyl rings oriented equatorially)[46] in the racemic form. A six-membered chelate ring formed by DAP and platinum (e.g., meso and racemic [Pt(2,2′-bipyridine)(DAP)]$^{2+}$) was also found to prefer the chair conformation with equatorial arrangement of the methyl groups in the meso form; however, a 70:30 conformer distribution (with the skew conformation having both *C*-Me's equatorial predominating over the chair conformation having equatorial/axial methyl groups) was found in the racemic form.[35]

In these previously studied complexes, substituents were present only on the chain bridging the two nitrogens. Six-membered chelate rings with substituents on the bridging chain and on the coordinated nitrogens, i.e., [$PtCl_2$(Et_2DAP)], have also been considered.[34] From molecular modeling studies restricted to the *RR*-Et_2DAP complexes (the analysis also applies to the *SS*-ligand), the conclusion was reached that the six-membered chelate ring preferred a chair conformation over a skew conformation regardless of the stereochemistries of the nitrogen centers (Et_2DAP differs from Me_2DAP only in having two *N*-Et's, instead of two *N*-Me's).[34] However, only one isomer was isolated and no detailed solution studies were performed. Therefore, no experimental information was available to assess the relative importance of intraligand and interligand steric interactions. An indication of the contribution of intra- and interligand interactions can be gained by ascertaining the preferred conformation in solution with NMR spectroscopy. We are in the favorable position to make such an assessment.

In our isomer **A**, both chair conformers (λ and δ) have equivalent dispositions of the *C*-Me's (equatorial/axial) but the

(42) Appleton, T. G.; Hall, J. R. *Inorg. Chem.* **1971**, *10*, 1717.
(43) Gollogly, J. L.; Hawkins, C. J. *Inorg. Chem.* **1972**, *11*, 156.
(44) Noji, M.; Okamoto, K.; Kidani, Y. *Chem. Lett.* **1979**, 741.
(45) Kammermeier, T.; Wiegrebe, W. *Arch. Farm. (Weinheim)* **1994**, *327*, 697.
(46) Interchange between the two puckers of a given conformation requires passing through another conformation.

conformers differ in the spatial disposition of the *N*-Me's (both equatorial in λ and both axial in δ). The clear preference for the conformation δ in solution indicates that, in the absence of other factors, the interactions between the *N*-Me's and the *cis* ligands are the leading factor favoring the bis-axial disposition of the *N*-Me's.[47] In support of this hypothesis, our MMD calculations on [$PtCl_2$(*SRRR*-Me_2DAP)] indicate that equatorial *N*-Me's experience nonbonded interactions with the *cis* chloride ligand. Thus, the δ-chair is more stable than the λ-chair conformation by 4.4 kcal/mol (Table 3). The λ-skew conformation would give a better positioning of the *C*-Me's (both equatorial) but a worse positioning of the *N*-Me's (equatorial/axial); the observed preference for the δ-chair conformation is therefore also an indication that interligand interactions (between *N*-Me's and *cis* halide ligands) are more stringent than intraligand interactions (between $C^{2,4}$-Me's). Finally, the λ-boat conformation, like the δ-chair, has equatorial/axial *C*-Me's and bis-axial *N*-Me's; however the eclipsed position of adjacent C and N atoms makes the λ-boat conformation higher in energy.

For isomer **B**, our NMR data suggest that the λ-skew conformation (equatorial *C*-Me's and axial *N*-Me's) is favored over both chair and boat conformations (axial/equatorial *C*-Me's and *N*-Me's). Our calculations agree; the λ-skew conformation is more stable than the chair conformations by 1.3 kcal/mol (Table 3), and the boat conformations were not among the low-energy structures. In contrast, for [$PtCl_2$(*RRRR*-Et_2DAP)] (Et_2-DAP = 2,4-bis(ethylamino)pentane), related to our isomer **B** of [$PtCl_2$(*RRRR*-Me_2DAP)], the chair conformation was predicted to be more stable.[34] Therefore, in order to determine if the difference arose from the method or from the change in the *N*-alkyl group, we performed calculations on [$PtCl_2$(*RRRR*-Et_2-DAP)] using our force field and found that the chair conformations were 1.3 kcal/mol lower in energy than the λ-skew conformation. Ignoring the additional *N*-Et carbons, we found our MMD structures of [$PtCl_2$(*RRRR*-Me_2DAP)] and [$PtCl_2$-(*RRRR*-Et_2DAP)] were essentially identical (rms_{heavy} = 0.04). Our calculations indicate that a chair conformation is favored for all three [$PtCl_2$(*RR*-Et_2DAP)] configurations, in agreement with the reported calculations.[34] Thus, there is an effect of changing the *N*-alkyl substituent; the *N*-Et's contributed more torsional deformation energy than *N*-Me's in the λ-skew conformation, favoring the chair conformations in [$PtCl_2$(*RRRR*-Et_2DAP)].

In isomer **C**, the chair conformations have axial/equatorial *C*-Me's and *N*-Me's (like the chair conformations of isomer **B**) but the skew conformation has either all *C*-Me's and *N*-Me's equatorial (λ) or all axial (δ); therefore, the chair conformation could represent the right compromise with respect to the skew conformations having either severe interligand interactions (λ) or severe intraligand interactions (δ). Our calculations suggest that a chair conformation is nearly 5 kcal/mol more stable than the δ-skew conformation; the λ-skew conformation was not observed in the energy-minimized structures. Also in this case, as in the case of isomer **A**, the relationships among methyl substituents in the boat conformation are similar to those seen in the chair conformation; however the eclipsed positioning of the groups attached to adjacent C and N atoms make the boat conformation less preferred.

Having discussed the compounds with the racemic diamine, we turn to the isomers with the meso ligand. We begin with isomer **E** because it has relatively straightforward properties.

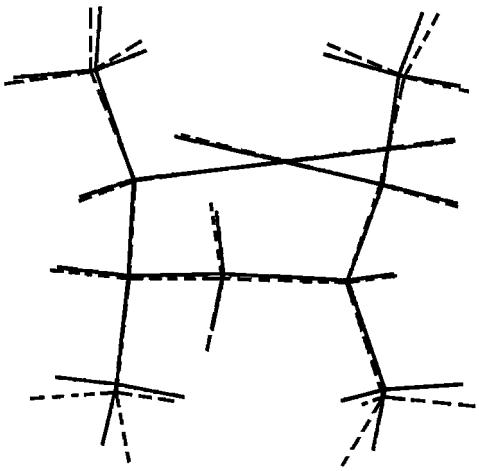

Figure 4. Superimposition of crystal (solid line) and calculated (dashed line) structures of [$PtCl_2$(*SRSR*-Me_2DAP)].

Since both intra- and interligand interactions are less severe in the λ-chair conformation (calculated to be >5 kcal/mol more stable than any other conformation; Table 3), it is obvious that this conformer will be the preferred one for **E**. The situation of this isomer is, in a sense, complementary to that of isomer **B**.

Finally, in isomer **D**, all the *C*-Me and the *N*-Me groups are axial in δ-chair or equatorial in λ-chair. Therefore interligand interactions are minimized in δ-chair (axial *N*-Me's) but intraligand interactions are minimized in λ-chair (equatorial *C*-Me's). In contrast, the skew conformation has axial/equatorial *C*-Me's and *N*-Me's. The situation is exactly reversed with respect to that seen for isomer **C**; therefore now the skew conformations could represent the right compromise with respect to the chair conformations, which have either severe interligand interactions (λ) or severe intraligand interactions (δ). Indeed, the NMR data indicate the skew conformations are favored in solution at room temperature. On the other hand, both the X-ray (solid) and MMD calculation structures are δ-chair. A solvent effect and an entropy factor (connected with fluxionality) could be the factors favoring the skew conformations in solution. The fluxional nature of **D** is supported by the calculations; a low-energy path to the interconversion of the skew conformers was found through the λ-boat conformation with equatorial *C*-Me's (minimal intraligand interactions) and axial *N*-Me's (minimal interligand interactions). The calculated low-energy barrier for skew to skew conformational change agrees with the experimental observation of fast exchange at −80 °C.

With the exception of isomer **D**, the calculated structures show good agreement with the structures predicted from the NMR results. Furthermore, the crystal structure of [$PtCl_2$(*SRSR*-Me_2DAP)] was compared to our calculated structure using two rms deviations: the platinum coordination plane (rms_{PtL_4}) deviation was 0.04 Å, while the heavy-atom (rms_{heavy}) deviation was 0.07 Å (Figure 4). By comparison, a force field that was recently developed and tested against 23 square planar platinum compounds gave rms_{PtL_4} deviations ranging from 0.01 to 0.17 Å and rms_{heavy} deviations ranging from 0.04 to 0.43 Å.[48] Therefore, our results indicate excellent agreement.

On the basis of X-ray data alone, it could be argued that attractive interactions between the Pt and the Me protons play a role in stabilizing the solid state structure. Interactions of

(47) It has already been reported that the energy differences between different stereoisomers are influenced by other groups coordinated to the Pt atom: Bosnich, B.; Sullivan, E. A. *Inorg. Chem.* **1975**, *14*, 2768.

(48) Cundari, T. R.; Fu, W.; Moody, E. W.; Slavin, L. L.; Snyder, L. A.; Sommerer, S. O.; Klinckman, T. R. *J. Phys. Chem.* **1996**, *100*, 18057.

this type have been suggested for many years[49] and more recently.[50] However, our MMD-calculated structure is very similar to the crystal structure despite the absence of a Pt−H attractive term in the AMBER force field. Therefore, such an interaction may be an additional but not an essential factor favoring this conformer. The X-ray structures also allow an estimate of the intraligand steric interactions. As expected, those between axial/axial *C*-Me's are more severe [shortest H···H distance 2.17(12) Å] than those between *N*-Me's [shortest H···H distance 2.40(14) Å]. Therefore both *N*-Me's can be accommodated in axial positions in order to avoid steric interaction with *cis* ligands.

Finally, we wish to point out that it has been possible to rank the different conformers by relative stability because, as already discussed, interconversion between conformers (chair, skew, and boat) requires only rotation about σ-bonds (skew/boat) or bond angle deformation [boat/chair (intermediate half-boat) and chair-skew (intermediate half-chair)]. Thus, this chemistry is under thermodynamic control. In contrast, we can not rank different diastereomers (**A**−**C** starting from *R*,*R*-Me_2DAP and **D**−**E** starting from *R*,*S*-Me_2DAP) by relative stability on the basis of isomer distribution in the preparations since the synthesis of these exchange-inert isomers is under kinetic control.

Acknowledgment. This work was supported by NIH Grant GM 29222 (to L.G.M.) and NATO Grant CRG 950376 (to L.G.M. and G.N.); MURST (contribution 40%), CNR, and EC (COST Chemistry Project D1/02/92) (to G.N.); and MURST (contribution 40%) and Università di Siena (contribution 60%) (to R.C.). NSF Grant ASC-9527186 supported our use of the Internet for remote collaborative research. Computations were performed at the Emerson Center (Emory). R.C. thanks Mr. Francesco Berrettini for the X-ray data collection at CIADS (Siena). Instrumentation at Emory was acquired with NIH and NSF grants. L.G.M. thanks the Japan Society for the Promotion of Science for a fellowship.

Supporting Information Available: Crystallographic data and refinement results (Table S1), atomic coordinates for $\mathbf{D}^{Cl}$ (Table S2) and $\mathbf{D}^{I}$ (Table S3), anisotropic displacement parameters for $\mathbf{D}^{Cl}$ (Table S4) and $\mathbf{D}^{I}$ (Table S6), and hydrogen atom parameters for $\mathbf{D}^{Cl}$ (Table S5) and $\mathbf{D}^{I}$ (Table S7) (7 pages). Ordering information is given on any current masthead page.

IC970704I

(49) Natile, G.; Maresca, L.; Cattalini, L. *J. Chem. Soc., Chem. Commun.* **1976**, 24. Natile, G.; Gasparrini, F.; Misiti, D.; Perego, G. *J. Chem. Soc., Dalton Trans.* **1977**, 1747. Natile, G.; Cattalini, L.; Gasparrini, F.; Caglioti, L. *J. Am. Chem. Soc.* **1979**, *101*, 498. Manotti-Lanfredi, A. M.; Tiripicchio, A.; Natile, G.; Gasparrini, F.; Galli, B. *Cryst. Struct. Commun.* **1979**, *8*, 611.

(50) Brammer, L.; Charnock, J. M.; Goggin, P. L.; Goodfellow, R. J.; Orpen, A. G.; Koetzle, T. F. *J. Chem. Soc., Dalton Trans.* **1991**, 1789.